TTMP vol 3 (1), 2026
doi: 10.30511/TTMP.2026.2081057.1069

Transactions in Theoretical and Mathematical Physics

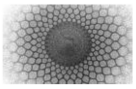

Analysis of the Viscous Laminar Flow in a Straight Pipe Based on the Complex Variable Finite Difference Method

Song-Chol Ri[1][a], **InGu Jo**[1], **Namsu Pak**[1]

[1] Faculty of Aerospace Engineering, Kim Chaek University of Technology, Pyongyang, Democratic People's Republic of Korea

Received: 16 December 2025 / Accepted: 21 February 2026 / Published: 22 February 2026

Abstract

The paper describes an efficient complex variable finite difference method (CVFDM) for calculating the two-dimensional potential flow, the viscous laminar flow in the straight pipe. The theoretical development is based on the generalization of the Cauchy-Riemann differential equation into the finite difference equation in terms of a complex variable to solve a two-dimensional boundary value problem. A numerical code is developed by this method and analytical solutions are obtained for illustrative problems. The validation of this method is confirmed through the analytical solutions for Pois-euille flow and Couette flow.

Keywords: Complex variable finite difference method; Cauchy-Riemann equation; Poiseuille flow; Couette flow

1 Introduction

The mathematical approach to an approximate method for solving the two-dimensional boundary value problems has been studied by many researchers, of which the complex variable boundary element method (CVBEM) and the complex variable finite element method (ZFEM) are typical methods.

Hromadka and Lai [1] derived a complex variable boundary element method (CVBEM) for solving numerically the problems governed by the two-dimensional Laplace equation. The potential flow past single and multicomponent airfoils in free air, in ground effect, in an infinite cascade, and in perforated wall wind tunnels, is calculated by the complex variable boundary element method algorithm [2]. Dumir *et al.* [3] presented a complex variable boundary element method for torsion of anisotropic cylindrical/prismatic bars whose longitudinal axis is normal to the plane of elastic symmetry of the bar. Satao [4] calculated the potential flow in the presence of thin objects based on the complex variable boundary element method. An accurate complex variable boundary element method is proposed for solving the two-dimensional boundary value problems governed by a steady-state advection-diffusion-reaction equation [5].

Tamayo *et al.* [6] applied a virtual crack extension technique using the complex variable finite element method (ZFEM) to the thermoplastic fracture problems. This virtual crack extension approach provided an accurate computation of the energy release rate as a byproduct of the complex variable finite element analysis without using energy conservation integrals. Millwater *et al.* [7] proposed the virtual crack extension method based on the complex variable finite element method and computed the energy release rate as a numerical derivative of the strain energy with respect to a crack extension using the complex Taylor series expansion method. Fielder *et al.* [8] detailed the application of the complex variable finite element method, ZFEM, to structures containing residual stresses. A thick-walled sphere model in which the residual stress field is induced by an autofrettage process, is considered. Since the results of ZFEM partial derivative results show high accuracy compared with standard finite element solutions, ZFEM is an effective step-size independent method for calculating shape, material, and loading sensitivities of structures subjected to residual stresses.

Restrepo *et al.* [9] combined the finite element method with the complex variable differentiation theory to calculate the first-order sensitivities for transient heat transfer equations accurately and reduced the computational time compared to traditional sensitivity analysis methods. Millwater *et al.* [10] computed accurate sensitivities with respect to the unknown parameters by solving an inverse finite element optimization problem using the complex variable finite

[a]Corresponding author: rsc83320@star-co.net.kp

element method, ZFEM, and proposed the use of full-field kinematic measurements to determine the constitutive material properties. Aaron Rios *et al.* [11] developed a complex variable transient thermo-mechanical element and used it to calculate accurate sensitivities of the thermal and stress time-dependent responses of a thick wall cylinder with temperature-dependent material properties using the complex Taylor series expansion (CTSE).

In this paper, the complex variable finite difference method (CVFDM) is introduced to analyze the two-dimensional potential problem. To calculate the velocity distribution of viscous laminar flow in a straight pipe, the Cauchy-Riemann differential equation is generalized to a complex finite difference equation and solve as a two-dimensional boundary value problem. The numerical results of CVFDM for the laminar flow velocity of a steady viscous fluid in a straight pipe are compared with the available analytical solutions to verify the proposed method.

2 The theoretical background of a complex variable finite difference method

The complex variable finite difference method is based on the Cauchy-Riemann equations. We will consider the complex variable function $F(z) = \psi + i\phi$ continued on boundary Γ of domain Ω (see Fig. 1), in which real part ψ and imaginary part ϕ satisfy the Cauchy-Riemann equations and Laplace's equation respectively.

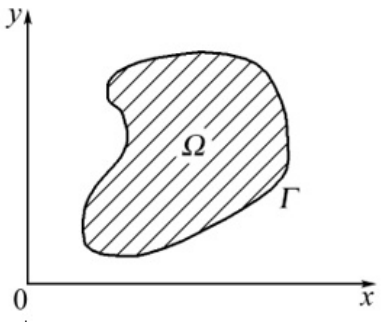

Fig. 1 Domain Ω enclosed by boundary curve Γ.

$$\begin{aligned}\frac{\partial\psi}{\partial x} &= \frac{\partial\phi}{\partial y},\\ \frac{\partial\psi}{\partial y} &= -\frac{\partial\phi}{\partial x}.\end{aligned} \tag{1}$$

Now we convert the Cauchy-Riemann equations into difference equations (see Fig. 2). The values of analytic function $F(z) = \psi + i\phi$ on the points A, B, C, D and O are described as $F_{i,j+1}$, $F_{i-1,j}$, $F_{i,j-1}$, $F_{i+1,j}$ and $F_{i,j}$.

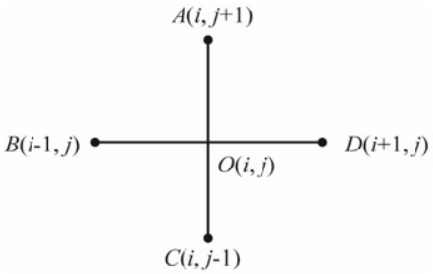

Fig. 2 Difference scheme.

By converting Eq. (1) into forward difference scheme,

$$\begin{aligned}\frac{\psi_{i+1,j}-\psi_{i,j}}{\Delta x} &= \frac{\phi_{i,j+1}-\phi_{i,j}}{\Delta y},\\ \frac{\psi_{i,j+1}-\psi_{i,j}}{\Delta y} &= -\frac{\phi_{i+1,j}-\phi_{i,j}}{\Delta x}.\end{aligned} \tag{2}$$

We introduce $\Delta y/\Delta x = k$ in the above equation. Then we deform the above equations, respectively,

$$\begin{aligned}\psi_{i+1,j}-\psi_{i,j} &= \frac{1}{k}(\phi_{i,j+1}-\phi_{i,j}),\\ \psi_{i,j+1}-\psi_{i,j} &= -k(\phi_{i+1,j}-\phi_{i,j}).\end{aligned} \tag{3}$$

We introduce the mathematical symbols *Re* (real part) and *Im* (imaginary part) on Eq. (3). Then

$$\begin{aligned}Re(F_{i+1,j}-F_{i,j}) &= \frac{1}{k}Im(F_{i,j+1}-F_{i,j}),\\ Re(F_{i,j+1}-F_{i,j}) &= -kIm(F_{i+1,j}-F_{i,j}).\end{aligned} \tag{4}$$

By accounting Eq. (4),

$$\begin{aligned}F_{i+1,j}-F_{i,j} =& Re(F_{i+1,j}-F_{i,j})+iIm(F_{i+1,j}-F_{i,j})\\ =& \frac{1}{k}Im(F_{i,j+1}-F_{i,j})-\frac{i}{k}Re(F_{i,j+1}-F_{i,j})\\ =& -\frac{i}{k}Re(F_{i,j+1}-F_{i,j})+\frac{1}{k}Im(F_{i,j+1}-F_{i,j})\\ =& -\frac{i}{k}\left[Re(F_{i,j+1}-F_{i,j})+iIm(F_{i,j+1}-F_{i,j})\right]\\ =& -\frac{i}{k}\left[(ReF_{i,j+1}+iImF_{i,j+1})-(ReF_{i,j}+iImF_{i,j})\right]\\ =& -\frac{i}{k}(F_{i,j+1}-F_{i,j}).\end{aligned} \tag{5}$$

By deforming the above equation,

$$F_{i+1,j}-F_{i,j} = -\frac{i}{k}(F_{i,j+1}-F_{i,j}), \tag{6}$$

or

$$kF_{i+1,j}-(k+i)F_{i,j}+iF_{i,j+1} = 0. \tag{7}$$

By deforming the difference scheme of Eq. (1) into backward difference scheme,

$$\frac{\psi_{i,j}-\psi_{i-1,j}}{\Delta x}=\frac{\phi_{i,j}-\phi_{i,j-1}}{\Delta y},$$
$$\frac{\psi_{i,j}-\psi_{i,j-1}}{\Delta y}=-\frac{\phi_{i,j}-\phi_{i-1,j}}{\Delta x}. \quad (8)$$

By arranging the above equation similarly,

$$kF_{i-1,j}-(k+i)F_{i,j}+iF_{i,j-1}=0. \quad (9)$$

By applying central difference to Eq. (1),

$$\frac{\psi_{i+1,j}-\psi_{i-1,j}}{2\Delta x}=\frac{\phi_{i,j+1}-\phi_{i,j-1}}{2\Delta y},$$
$$\frac{\psi_{i,j+1}-\psi_{i,j-1}}{2\Delta y}=-\frac{\phi_{i+1,j}-\phi_{i-1,j}}{2\Delta x}. \quad (10)$$

By arranging the above equation,

$$k(F_{i+1,j}-F_{i-1,j})+i(F_{i,j+1}-F_{i,j-1})=0. \quad (11)$$

We will consider one method of solving Eqs. (7), (9) and (11). We divide rectangular element EFGH by using a horizontal line BD and a vertical AC, make 4 elementary rectangles such as EBOA, AODH, BFCO and OCGD (see Fig. 3).

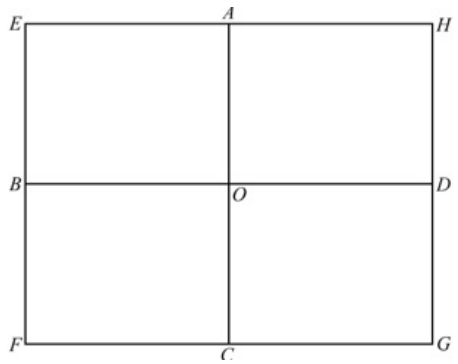

Fig. 3 Dividing of rectangular element.

Here $F_{i,j+1}(A)$, $F_{i-1,j}(B)$, $F_{i,j-1}(C)$, $F_{i+1,j}(D)$, $F_{i-1,j+1}(E)$, $F_{i-1,j-1}(F)$, $F_{i+1,j-1}(G)$, $F_{i+1,j+1}(H)$ and $F_{i,j}(O)$ are values of complex function on the angular points A,B,C,D,E,F,G,H and O,

$$F_A=\psi_{i,j+1}+i\phi_{i,j+1},$$
$$F_B=\psi_{i-1,j}+i\phi_{i-1,j},$$
$$F_C=\psi_{i,j-1}+i\phi_{i,j-1},$$
$$F_D=\psi_{i+1,j}+i\phi_{i+1,j},$$
$$F_E=\psi_{i-1,j+1}+i\phi_{i-1,j+1},$$
$$F_F=\psi_{i-1,j-1}+i\phi_{i-1,j-1},$$
$$F_G=\psi_{i+1,j-1}+i\phi_{i+1,j-1},$$
$$F_H=\psi_{i+1,j+1}+i\phi_{i+1,j+1},$$
$$F_O=\psi_{i,j}+i\phi_{i,j},$$

where $\psi_{i,j+1}$, $\psi_{i-1,j}$, $\psi_{i,j-1}$, $\psi_{i+1,j}$, $\psi_{i-1,j+1}$, $\psi_{i-1,j-1}$, $\psi_{i+1,j-1}$ and $\psi_{i+1,j+1}$ are 8 known, and $\psi_{i,j}$, $\phi_{i,j}$, $\phi_{i,j+1}$, $\phi_{i-1,j}$, $\phi_{i,j-1}$, $\phi_{i+1,j}$, $\phi_{i-1,j+1}$, $\phi_{i-1,j-1}$, $\phi_{i+1,j-1}$ and $\phi_{i+1,j+1}$ are 10 unknowns. We make the matrix form as follows to solve the 1^{st} polynomial systems of equations with 10 unknowns.

$$\begin{pmatrix} -k & 0 & 0 & 0 & -1 & 1 & 0 & 0 & 0 & 0\\ -1 & 0 & k & 0 & 0 & -k & 0 & 0 & 0 & 0\\ -k & 0 & 0 & 0 & 0 & 1 & -1 & 0 & 0 & 0\\ -1 & 0 & 0 & 0 & 0 & -k & 0 & 0 & k & 0\\ 0 & 0 & 0 & 0 & 0 & 0 & 0 & 0 & -1 & 1\\ 0 & 0 & 0 & 0 & 0 & 0 & k & 0 & 0 & -k\\ 0 & 1 & -1 & 0 & 0 & 0 & 0 & 0 & 0 & 0\\ 0 & -k & 0 & 0 & k & 0 & 0 & 0 & 0 & 0\\ 0 & 1 & 0 & -1 & 0 & 0 & 0 & 0 & 0 & 0\\ 0 & -k & 0 & 0 & 0 & 0 & 0 & k & 0 & 0 \end{pmatrix}$$
$$\times\begin{pmatrix} \psi_{ij}\\ \phi_{i-1,j-1}\\ \phi_{i-1,j}\\ \phi_{i-1,j+1}\\ \phi_{i,j-1}\\ \phi_{i,j}\\ \phi_{i,j+1}\\ \phi_{i+1,j-1}\\ \phi_{i+1,j}\\ \phi_{i+1,j+1} \end{pmatrix}=\begin{pmatrix} -k\psi_{i-1,j}\\ -\psi_{i,j-1}\\ -k\psi_{i+1,j}\\ -\psi_{i,j+1}\\ -k\psi_{i,j+1}+k\psi_{i+1,j+1}\\ \psi_{i+1,j+1}-\psi_{i+1,j}\\ -k\psi_{i,j-1}+k\psi_{i-1,j-1}\\ \psi_{i-1,j-1}-\psi_{i-1,j}\\ -k\psi_{i+1,j-1}+k\psi_{i-1,j-1}\\ \psi_{i-1,j-1}-\psi_{i-1,j+1} \end{pmatrix}. \quad (12)$$

We can calculate the unknowns ψ and ϕ in the domain and on the boundary by solving these matrix equations. We will compare an error between Cauchy-Riemann differential equation and Laplace differential equation. The difference form of Laplace equation can be expressed as

$$\frac{\psi_{i+1,j}-2\psi_{i,j}+\psi_{i-1,j}}{h^2}+\frac{\psi_{i,j+1}-2\psi_{i,j}+\psi_{i,j-1}}{k^2}=\overline{L_1(\psi)} \quad (13)$$

where h is a x-direction length of elementary rectangle, k is y-direction length of elementary rectangle. By introducing equation $k=\delta h$

$$\overline{L_1(\psi)}=\frac{1}{h^2}\Big[(\psi_{i+1,j}-2\psi_{i,j}+\psi_{i-1,j})+\frac{1}{\delta^2}(\psi_{i,j+1}-2\psi_{i,j}+\psi_{i,j-1})\Big]. \quad (14)$$

By expressing the error between Eq. (14) and Laplace equation as $R_1(\psi)$,

$$R_1(\psi)=\overline{L_1(\psi)}-L_1(\psi),$$

where $L_1(\psi)$ is an error of Laplace differential equation. Therefore,

$$L_1(\psi)=\frac{\partial^2\psi}{\partial x^2}+\frac{\partial^2\psi}{\partial y^2},$$

Because $L_1(\psi)=0$,

$$\begin{aligned}R_1(\psi)=&\frac{1}{h^2}\Big[\Big(\psi_{i,j}+h\frac{\partial\psi_{i,j}}{\partial x}+\frac{h^2}{2!}\frac{\partial^2\psi_{i,j}}{\partial x^2}+\frac{h^3}{3!}\frac{\partial^3\psi_{i,j}}{\partial x^3}\\&+\frac{h^4}{4!}\frac{\partial^4\psi_{i,j}}{\partial x^4}+\frac{h^5}{5!}\frac{\partial^5\psi_{i,j}}{\partial x^5}+\frac{h^6}{6!}\frac{\partial^6\psi_{i,j}}{\partial x^6}-2\psi_{i,j}\\&+\psi_{i,j}-h\frac{\partial\psi_{i,j}}{\partial x}+\frac{h^2}{2!}\frac{\partial^2\psi_{i,j}}{\partial x^2}-\frac{h^3}{3!}\frac{\partial^3\psi_{i,j}}{\partial x^3}\\&+\frac{h^4}{4!}\frac{\partial^4\psi_{i,j}}{\partial x^4}-\frac{h^5}{5!}\frac{\partial^5\psi_{i,j}}{\partial x^5}+\frac{h^6}{6!}\frac{\partial^6\psi_{i,j}}{\partial x^6}\Big)\\&+\frac{1}{\delta^2}\Big(\psi_{i,j}+k\frac{\partial\psi_{i,j}}{\partial y}+\frac{k^2}{2!}\frac{\partial^2\psi_{i,j}}{\partial y^2}+\frac{k^3}{3!}\frac{\partial^3\psi_{i,j}}{\partial y^3}\\&+\frac{k^4}{4!}\frac{\partial^4\psi_{i,j}}{\partial y^4}+\frac{k^5}{5!}\frac{\partial^5\psi_{i,j}}{\partial y^5}+\frac{k^6}{6!}\frac{\partial^6\psi_{i,j}}{\partial y^6}-2\psi_{i,j}\\&+\psi_{i,j}-k\frac{\partial\psi_{i,j}}{\partial y}+\frac{k^2}{2!}\frac{\partial^2\psi_{i,j}}{\partial y^2}-\frac{k^3}{3!}\frac{\partial^3\psi_{i,j}}{\partial y^3}\\&+\frac{k^4}{4!}\frac{\partial^4\psi_{i,j}}{\partial y^4}-\frac{k^5}{5!}\frac{\partial^5\psi_{i,j}}{\partial y^5}+\frac{k^6}{6!}\frac{\partial^6\psi_{i,j}}{\partial y^6}\Big)\Big]\\&+\mathscr{O}(h^6).\end{aligned}$$

Then,

$$\begin{aligned}R_1(\psi)=&\frac{1}{h^2}\Big[\Big(\frac{\partial^2\psi_{i,j}}{\partial x^2}+\frac{\partial^2\psi_{i,j}}{\partial y^2}\Big)\frac{h^2}{2}\\&+\Big(\frac{\partial^4\psi_{i,j}}{\partial x^4}+\delta^2\frac{\partial^4\psi_{i,j}}{\partial y^4}\Big)\frac{h^4}{12}\\&+\Big(\frac{\partial^6\psi_{i,j}}{\partial x^6}+\delta^4\frac{\partial^6\psi_{i,j}}{\partial y^6}\Big)\frac{h^6}{36}\Big]+\mathscr{O}(h^6),\end{aligned}\tag{15}$$

where

$$\frac{\partial^2\psi_{i,j}}{\partial x^2}=-\frac{\partial^2\psi_{i,j}}{\partial y^2},\qquad\frac{\partial^4\psi_{i,j}}{\partial x^4}=\frac{\partial^4\psi_{i,j}}{\partial y^4},$$
$$\frac{\partial^6\psi_{i,j}}{\partial x^6}=-\frac{\partial^6\psi_{i,j}}{\partial y^6}.$$

Thus,

$$\begin{aligned}R_1(\psi)=&\frac{h^2}{12}(1+\delta^2)\frac{\partial^4\psi_{i,j}}{\partial x^4}+\frac{h^4}{36}(1-\delta^4)\frac{\partial^6\psi_{i,j}}{\partial x^6}\\&+\mathscr{O}(h^6).\end{aligned}\tag{16}$$

If we assume $\delta=1$, then one can easily obtain

$$R_1(\psi)=\frac{h^2}{6}\frac{\partial^4\psi_{i,j}}{\partial x^4}+\mathscr{O}(h^6).\tag{17}$$

Therefore, the error of Laplace differential equation is in the h^2 order. Now we consider an error of Cauchy-Riemann differential equation on the rectangular grid. By applying a forward differential scheme on and backward differential scheme on respectively,

$$\begin{aligned}\frac{\psi_{i+1,j}-\psi_{i,j}}{h}&=\frac{\phi_{i,j}-\phi_{i,j-1}}{k},\\\frac{\phi_{i,j}-\phi_{i-1,j}}{h}&=-\frac{\psi_{i,j+1}-\psi_{i,j}}{k}.\end{aligned}\tag{18}$$

From the above equation,

$$\begin{aligned}\overline{L_2(\psi)}=&\frac{1}{h}\Big[(\psi_{i+1,j}-2\psi_{i,j}+\psi_{i-1,j})\\&+\frac{1}{\delta^2}(\psi_{i,j+1}-2\psi_{i,j}+\psi_{i,j-1})\Big].\end{aligned}\tag{19}$$

By expressing an error of Cauchy-Riemann differential equation as $R_2(\psi)$,

$$R_2(\psi)=\overline{L_2(\psi)}-L_2(\psi),$$

where $L_2(\psi)$ is an error of Cauchy-Riemann differential equation $L_2(\psi)=0$. Thus,

$$\begin{aligned}R_2(\psi)=\overline{L_2(\psi)}=&\frac{1}{h}\Big[(\psi_{i+1,j}-2\psi_{i,j}+\psi_{i-1,j})\\&+\frac{1}{\delta^2}(\psi_{i,j+1}-2\psi_{i,j}+\psi_{i,j-1})\Big].\end{aligned}\tag{20}$$

By using the Tailor series around point (x_i,y_j) of the above equation,

$$\begin{aligned}R_2(\psi)=&\frac{h^3}{12}(1+\delta^2)\frac{\partial^4\psi_{i,j}}{\partial x^4}+\frac{h^5}{36}(1-\delta^4)\frac{\partial^6\psi_{i,j}}{\partial x^6}\\&+\mathscr{O}(h^6).\end{aligned}\tag{21}$$

We can know that the error of Cauchy-Riemann differential equation is the h^3 order from Eq. (21).

Considering a value of $e=R_2(\psi)/R_1(\psi)$, we can know that an error of Cauchy-Riemann differential equation is h times smaller than an error of Laplace differential equation. Generally the error changes with the form of difference scheme. By using the central difference scheme respectively error $R'(\psi)$ is the same as equation (22).

$$\begin{aligned}R'(\psi)=R_2(\psi)=&\frac{8h^3}{12}(1+\delta^2)\frac{\partial^4\psi_{i,j}}{\partial x^4}\\&+\frac{32h^5}{36}(1-\delta^4)\frac{\partial^6\psi_{i,j}}{\partial x^6}+\mathscr{O}(h^6).\end{aligned}\tag{22}$$

From the above equation, we can know that error is 8 times bigger than above error. We will introduce a relaxation method of elevating the convergence of a complex variable difference solution.

$$kF_{i+1,j}-(k+i)F_{i,j}+iF_{i,j+1}=0.\tag{23}$$

By expressing the iterative order as n, the above equation is the same as follows:

$$kF^{n-1}_{i+1,j}-(k+i)F^{n}_{i,j}+iF^{n-1}_{i,j+1}=0.\tag{24}$$

By putting $k=1$ to arrange the above equation simply,

$$F^{n-1}_{i+1,j}-(1+i)F^{n-1}_{i,j}+iF^{n-1}_{i,j+1}=(1+i)(F^{n}_{i,j}-F^{n-1}_{i,j}).\tag{25}$$

By dividing real and imaginary parts in Eq. (22), we then find that

$$\begin{aligned}\psi_{i+1,j}^{n-1}-\psi_{i,j}^{n-1}+\phi_{i,j}^{n-1}-\phi_{i,j+1}^{n-1}&\\ =\psi_{i,j}^{n}-\psi_{i,j}^{n-1}-(\phi_{i,j}^{n}-\phi_{i,j}^{n-1}),&\\ \psi_{i,j+1}^{n-1}-\psi_{i,j}^{n-1}+\phi_{i+1,j}^{n-1}-\phi_{i,j}^{n-1}&\\ =\psi_{i,j}^{n}-\psi_{i,j}^{n-1}-(\phi_{i,j}^{n}-\phi_{i,j}^{n-1}),&\end{aligned}\tag{26}$$

where $\psi_{i,j}^{n}$, $\phi_{i,j}^{n}$, $\psi_{i,j}^{n-1}$ and $\phi_{i,j}^{n-1}$ are values in other fields of point (i,j).

Let's introduce a new free parameter t, express iterative order by it and deform into the following differential equation.

$$\begin{aligned}\frac{\partial\psi}{\partial x}-\frac{\partial\phi}{\partial y}&=\frac{\partial\psi}{\partial t}-\frac{\partial\phi}{\partial t},\\ \frac{\partial\psi}{\partial y}+\frac{\partial\phi}{\partial x}&=\frac{\partial\psi}{\partial t}+\frac{\partial\phi}{\partial t}.\end{aligned}\tag{27}$$

By introducing the following equations,

$$\psi(x,y,t)=k(t)G(x,y),\qquad \phi(x,y,t)=k(t)H(x,y),\tag{28}$$

and by substituting Eq. (28) into Eq. (27), we then obtain

$$\begin{aligned}k(t)\Big(\frac{\partial G}{\partial x}-\frac{\partial H}{\partial y}\Big)&=\frac{\partial k(t)}{\partial t}(G-H),\\ k(t)\Big(\frac{\partial G}{\partial y}+\frac{\partial H}{\partial x}\Big)&=\frac{\partial k(t)}{\partial t}(G+H).\end{aligned}\tag{29}$$

Then

$$\frac{\left(\frac{\partial G}{\partial x}-\frac{\partial H}{\partial y}\right)}{G-H}=\frac{\left(\frac{\partial G}{\partial y}+\frac{\partial H}{\partial x}\right)}{G+H}=\frac{k'(t)}{k(t)}=-\lambda_m^2.\tag{30}$$

From Eq. (30) we find that

$$k'(t)+\lambda_m^2 k(t)=0.\tag{31}$$

and

$$\begin{aligned}\frac{\partial G}{\partial x}-\frac{\partial H}{\partial y}+\lambda_m^2(G-H)&=0,\\ \frac{\partial G}{\partial y}+\frac{\partial H}{\partial x}+\lambda_m^2(G+H)&=0.\end{aligned}\tag{32}$$

By introducing the following equations,

$$G(x,y)=A(x)B(y),\qquad H(x,y)=C(x)D(y).\tag{33}$$

By substituting Eq. (33) into Eq. (32), we then have

$$\frac{dA}{dx}.\frac{1}{C}+\lambda_m^2\frac{A}{C}=\frac{1}{B}.\frac{dD}{dy}+\lambda_m^2\frac{D}{B}.\tag{34}$$

Because left side and right side of Eq. (34) are functions about x and y, they are constant m.

$$\begin{aligned}\frac{dA}{dx}+\lambda_m^2A-Cm&=0,\\ \frac{dD}{dy}+\lambda_m^2D-Bm&=0.\end{aligned}\tag{35}$$

By substituting Eq. (33) into Eq. (35), Eq. (33) equals as follows:

$$\frac{1}{D}.\frac{dB}{dy}+\lambda_m^2\frac{B}{D}=-\frac{1}{A}.\frac{dC}{dx}-\lambda_m^2\frac{C}{A}.\tag{36}$$

Because left side and right side in Eq. (36) are functions of x and y, they are constant n. Then above equation equals as follows:

$$\begin{aligned}\frac{dB}{dy}+\lambda_m^2B-Dn&=0,\\ \frac{dC}{dx}+\lambda_m^2C+An&=0.\end{aligned}\tag{37}$$

By deciding A, B, C and D from Eqs. (35) and (37), we can decide $G(x,y)$ and $H(x,y)$ from Eq. (33). Thus, we can get ψ and ϕ of Eq. (33).

$$\begin{aligned}\psi(x,y,t)&=G_0(x,y)+\sum_{m=1}^{\infty}A_m e^{-\lambda_m^2 t}G_m(x,y),\\ \phi(x,y,t)&=H_0(x,y)+\sum_{m=1}^{\infty}B_m e^{-\lambda_m^2 t}H_m(x,y).\end{aligned}\tag{38}$$

In Eq. (38), $G_0(x,y)$ and $H_0(x,y)$ are solutions of the following equations

$$\begin{aligned}\frac{\partial G}{\partial x}-\frac{\partial H}{\partial y}&=0,\\ \frac{\partial G}{\partial y}+\frac{\partial H}{\partial x}&=0.\end{aligned}\tag{39}$$

The second term of right side in Eq. (38) is an error of iterative calculation. The value of this term is 0 on $t\to\infty$.

$$\begin{aligned}lim_{t\to\infty}\psi(x,y,t)&=G_0(x,y),\\ lim_{t\to\infty}\phi(x,y,t)&=H_0(x,y).\end{aligned}\tag{40}$$

Thus, the result of simple iterative calculation converges to solution of Cauchy-Riemann differential equations from above result we can know that numerical calculation has convergence. The convergence is decided by power λ_1^2 of the second term in right side of Eq. (38), where λ_1^2 is the smallest eigenvalue. The greater this power is, the higher the convergence is. The above eigenvalue equals λ_1^2nh.

We can see that convergence is inversely proportional to the step size. That is proportional to the total number of grid points. Thus, power represents the convergence of *nth* iterative calculation. Thus, λ_1^2h shows the increment of convergent velocity in the first iterative calculation.

3 Numerical results on the viscous laminar flow in the straight pipe

We have considered the new method of calculating the velocity of Poiseuille flow and Couette flow by using the complex variable finite difference method in this paper. We consider *N-S* equation in order to calculate the steady laminar flow velocity of viscous fluid in the straight pipe,

$$\frac{dV}{dt} = \frac{\partial V}{\partial t} + (\nabla.V)V = K - \frac{1}{\rho} gradP + \gamma.\nabla^2 V. \tag{41}$$

$$\begin{aligned}
&\frac{\partial u}{\partial t} + u\frac{\partial u}{\partial x} + v\frac{\partial u}{\partial y} + w\frac{\partial u}{\partial z} = X - \frac{1}{\rho}.\frac{\partial p}{\partial x} \\
&\qquad + \frac{\mu}{\rho}\left(\frac{\partial^2 u}{\partial x^2} + \frac{\partial^2 u}{\partial y^2} + \frac{\partial^2 u}{\partial z^2}\right), \\
&\frac{\partial v}{\partial t} + u\frac{\partial v}{\partial x} + v\frac{\partial v}{\partial y} + w\frac{\partial v}{\partial z} = Y - \frac{1}{\rho}.\frac{\partial p}{\partial y} \\
&\qquad + \frac{\mu}{\rho}\left(\frac{\partial^2 v}{\partial x^2} + \frac{\partial^2 v}{\partial y^2} + \frac{\partial^2 v}{\partial z^2}\right), \\
&\frac{\partial w}{\partial t} + u\frac{\partial w}{\partial x} + v\frac{\partial w}{\partial y} + w\frac{\partial w}{\partial z} = Z - \frac{1}{\rho}.\frac{\partial p}{\partial z} \\
&\qquad + \frac{\mu}{\rho}\left(\frac{\partial^2 w}{\partial x^2} + \frac{\partial^2 w}{\partial y^2} + \frac{\partial^2 w}{\partial z^2}\right),
\end{aligned} \tag{42}$$

where V is the vector of velocity, γ is the kinematical viscosity $\gamma = \mu/\rho$, μ is the viscosity, ρ is the density of fluid and $K = X\hat{i} + Y\hat{j} + Z\hat{k}$.

We assume that the incompressible fluid with viscosity μ moves along constant direction in the straight pipe with different section (see Fig. 4). We set up z-axis as flow direction, while the velocity of x-axis and y-axis is 0. Thus $\partial w/\partial z = 0$, then w is a function about x and y. By applying the motion equation, we get the following equation.

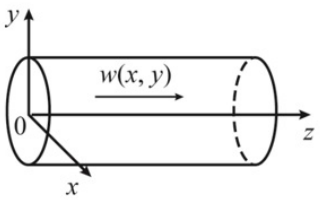

Fig. 4 Flow along z-direction in the straight pipe with different section.

$$\frac{\partial p}{\partial x} = 0, \quad \frac{\partial p}{\partial y} = 0, \quad \frac{\partial p}{\partial z} = \mu\left(\frac{\partial^2 w}{\partial x^2} + \frac{\partial^2 w}{\partial y^2}\right). \tag{43}$$

Here we know that pressure p is only a function of z from first and second equation. Considering the right side of third equation is a function of x and y, we can get a pressure gradient along z-axis in the straight pipe as $\partial p/\partial z = J$ (J is constant). Thus,

$$\frac{\partial^2 w}{\partial x^2} + \frac{\partial^2 w}{\partial y^2} = \frac{J}{\mu}, \tag{44}$$

and we consider that the fluid satisfies the equation $w = 0$ on the wall of pipe. According to it, we can get the distribution of the velocity along x-axis and y-axis,

$$w = \varphi - \frac{J}{4\mu}(x^2 + y^2), \tag{45}$$

where $\varphi(x, y)$ is the harmonic function of satisfying Laplace differential equation. Substituting w into the motion equation, we get the equation about φ.

$$\frac{\partial^2 \varphi}{\partial x^2} + \frac{\partial^2 \varphi}{\partial y^2} = 0. \tag{46}$$

The value of the function satisfying Eq. (46) is expressed as follows:

$$\varphi^2 = \frac{J}{4\mu}(x^2 + y^2). \tag{47}$$

Because the velocity of a Poiseuille flow is 0 on the boundary of the wall, we can calculate the velocity of the steady laminar flow in the straight pipe.

$$w = \varphi - \frac{J}{4\mu}(x^2 + y^2). \tag{48}$$

Therefore, we can get φ by the complex variable finite difference method and then get the velocity w from Eq. (48). Because a pressure gradient along z-axis of Poiseuille flow in the straight pipe is not 0, a pressure gradient along z-axis of Couette flow in the straight pipe is 0. Therefore, the velocity of Poiseuille flow in the straight pipe satisfies a Poisson equation of non-homogeneous second-order partial differential equation. On the other hand, the velocity of Couette flow in the straight pipe satisfies a Laplace equation of the homogeneous second-order partial differential equation.

The approximate velocity of Poiseuille flow and Couette flow in the straight pipe can be easily solved with a computer code made in MATHCAD. Numerical results can be obtained for any straight pipe with a different section, but in order to validate the computer code, we consider a particular case, the problem of approximate velocity of Poiseuille flow and Couette flow in the straight pipe with a rectangular section. It has great importance because it offers us the possibility to make a comparison between the exact solution and the numerical one.

First, we calculate the velocity of Couette flow in the straight pipe by using the present method. The velocity of Couette flow in the straight pipe with rectangular section is represented as a cubic graph. (see Fig. 5) and the different sectional graphics (see Figs. 6, 7 and 8). The width of the rectangular section in the straight pipe is 2400, and

the length of the rectangular section in the straight pipe is 800. The velocities of Couette flow on 4 borders of rectangular section have different sizes respectively, that is, the magnitudes of velocity w on every border are 1000, 2000, 3000 and 4000. After considering the magnitudes of velocity based on the cubic graph, the approximate velocity w of Couette flow in the straight pipe with rectangular section from the calculated results, we can see that the larger the velocity magnitude at the boundary, the larger the cubic gradient of velocity w in the Couette flow in a straight pipe with a rectangular section. Specifically, this paper presents detailed data on the approximate velocities of Couette flow at every section along the width direction. According to this, we can see that the change of velocity of Couette flow from a width of $x = 440$ to $x = 2000$ is not large, and the form of the velocity curves changes very little compared with changes in width.

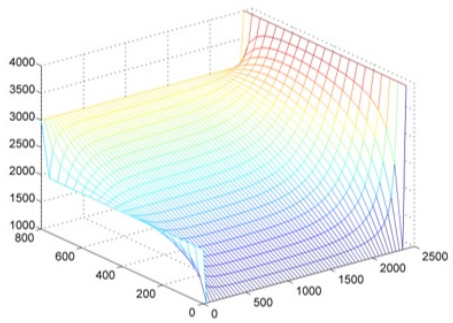

Fig. 5 The approximate velocity w of Couette flow in the straight pipe with rectangular section.

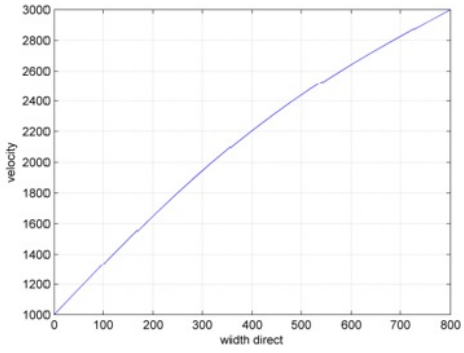

Fig. 6 The approximate velocity w of Couette flow on width $x = 440$ of rectangular section.

Second, we calculate the velocity in Poiseuille flow in a straight pipe using the present method. The size of the velocity w of Poiseuille flow in the straight pipe with rectangular section by the complex variable finite element method is

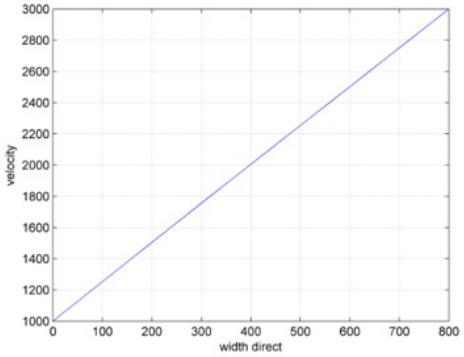

Fig. 7 The approximate velocity w of Couette flow on width $x = 1240$ of rectangular section.

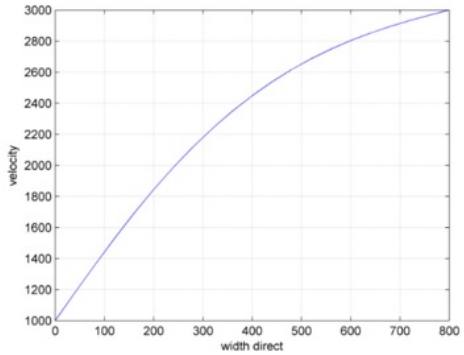

Fig. 8 The approximate velocity w of Couette flow on the width $x = 2000$ of rectangular section.

represented in the cubic graphics (see Fig. 9) and in different sectional graphics respectively (see Figs. 9, 10 and 11). In this paper, we have calculated the velocity w of Poiseuille flow in the straight pipe with rectangular section in the case of pressure gradient $J = \partial p/\partial z = -10$. The width of the rectangular section in the straight pipe is 2400, and the length of the rectangular section in the straight pipe is 800. The velocities of Poiseuille flow on 4 borders of rectangular section have different sizes respectively, that is, the magnitudes of velocity w on every border are 0. After considering the magnitudes of velocity based on the cubic graph of the approximate velocity w of Poiseuille flow in the straight pipe with rectangular section from the calculated results, we can see that the larger the magnitude of velocity on the border, the larger the cubic gradient of velocity w of Poiseuille flow in the straight pipe with rectangular section. Specifically, detailed data on the approximate velocities of Poiseuille flow at every section along the width are presented in this paper. According to this, we can see that the change of velocity of Poiseuille flow from a width of $x = 440$ to $x = 2000$ is not large, and the form of the velocity curves changes very little compared with changes in width. Figs. 10, 11 and 12 show that profiles of velocity curve are reasonably smooth The computational procedure appears to be appropriate for a straight pipe with a different section.

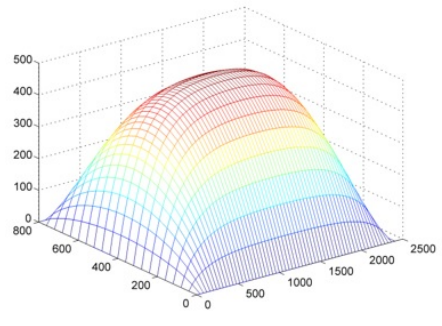

Fig. 9 The approximate velocity w of Poiseuille flow in the straight pipe with rectangular section.

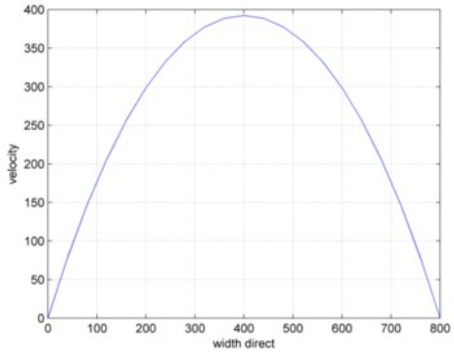

Fig. 10 The approximate velocity w of Poiseuille flow on width $x = 440$ of rectangular section.

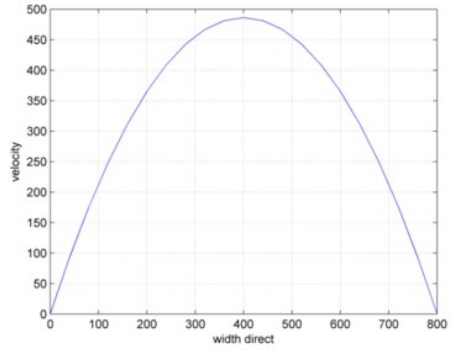

Fig. 11 The approximate velocity w of Poiseuille flow on width $x = 1240$ of rectangular section.

4 Conclusion

In this paper, the complex variable finite difference method (CVFDM) is applied to analyze the viscous laminar flow in a straight pipe. The Cauchy-Riemann differential equation for solving the two-dimensional potential problem is generalized to a complex finite difference equation. To verify the accuracy of the proposed method, the analytical solutions for Poiseuille and Couette flows are obtained.

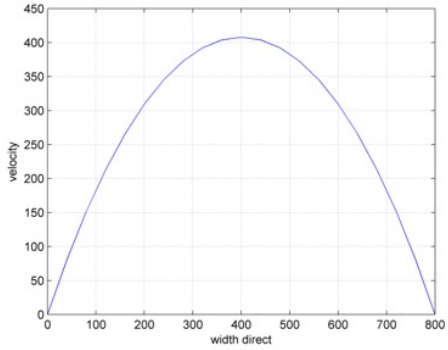

Fig. 12 The approximate velocity w of Poiseuille flow on width $x = 2000$ of rectangular section.

The CVFDM has been demonstrated to be an efficient technique for solving the two-dimensional boundary value problem. The advantages of CVFDM include easy grid generation, fast computation, and high computational accuracy. The CVFEM can also be applied to various physical phenomena that satisfy the Cauchy-Riemann equation.

Declaration of competing interest

The authors declare that they have no conflict of interest.

Funding

This work was supported by ongoing institutional funding. No additional grants to carry out or direct this particular research were obtained.

Author contributions

All authors contribute to the study conception and design. Material preparation, data collection and analysis were performed by Song-Chol Ri, InGu Jo and Namsu Pak. The first draft of the manuscript was written by Song-Chol Ri and all authors commented on previous versions of the manuscript. All authors read and approved the final manuscript.

Acknowledgements The authors would like to express their gratitude to the handling editor and reviewers for their constructive comments.

References

1. T. V. Hromadka, C. Lai, *The complex variable boundary element method in engineering analysis*, (Springer-Verlag, Berlin 1987)
2. M. Mokry, AIAA Journal, **29**, no. 12, 2027 (1991). DOI: https://doi.org/10.2514/3.10836
3. P. C. Dumir, R. Kumar, Appl. Math. Modelling, **17**, 80 (1993). DOI: https://doi.org/10.1016/0307-904X(93)90096-Y

4. K. Sato, Comput. Methods in Appl. Mech. Eng., **192**, 1421 (2003)
5. X. Wang, Whye-Teong Ang, Appl. Math. Comput., **321**, 731 (2018). DOI: https://doi.org/10.1016/j.amc.2017.10.042
6. D. R. Tamayo, A. Montoya, H. Millwater, Eng. Fract. Mech., **192**, 328 (2018). DOI: https://doi.org/10.1016/j.engfracmech.2017.12.013
7. H. Millwater, D. Wagner, A. Montoya, Eng. Fract. Mech., **162**, 95 (2016). DOI: https://doi.org/10.1016/j.engfracmech.2016.04.002
8. R. Fielder, A. Montoya, H. Millwater, P. Golden, Int. J. Mech. Sci., **133**, 112 (2017). DOI: https://doi.org/10.1016/j.ijmecsci.2017.08.035
9. D. Restrepo, et al., Appl. Sci., **12**, no 5, 2738 (2022). DOI: https://doi.org/10.3390/app12052738
10. H. Millwater, et al., Int. J. Solids Struct., **243**, 111545 (2022). DOI: https://doi.org/10.1016/j.ijsolstr.2022.111545
11. G. A. Rios, J. S. R. Tabares, A. Montoya, D. Restrepo, H. Millwater, J. Therm. Stress., **45**, no 5, 341 (2022). DOI: https://doi.org/10.1080/01495739.2022.2034976